



Recombinant adeno-associated virus BMP-4/7 fusion gene confers ossification activity in rabbit bone marrow stromal cells

S.H. Yuan, C.B. Gao, C.U. Yin, Z.G. Yin

Department of Orthopedics, First Hospital of Harbin Medical University, Harbin, China

Corresponding author: Z.G. Yin
E-mail: zhenggangbi@126.com

Genet. Mol. Res. 11 (3): 3105-3114 (2012)
Received February 13, 2012
Accepted July 24, 2012
Published August 31, 2012
DOI <http://dx.doi.org/10.4238/2012.August.31.8>

ABSTRACT. The biological effects of transfection of an adeno-associated virus (AAV) vector with bone morphogenetic proteins 4 and 7 (BMP-4/7) fusion gene (AAV-BMP-4/7) were determined in rabbit bone marrow stromal cells (BMSCs). BMP-4 and BMP-7 genes were obtained through one-step reverse transcriptase polymerase chain reaction from human placental cells. The BMP-4/7 fusion gene was then generated through recombination. Rabbit BMSCs were transfected with the recombinant AAV vectors carrying AAV-BMP-4/7 with multiplicity of infection values. Cell growth curves were drawn to evaluate the biological effects of AAV-BMP-4/7 on cell activity. The transfection efficiency was measured using a 3-(4,5-dimethylthiazol-2-yl)-2,5-diphenyltetrazolium bromide assay. The ossification of cells was evaluated by observing alkaline phosphatase (ALP) and osteocalcin (OC) activity after transfection for 7 and 14 days. The cells were then transfected with AAV-BMP-4/7 and AAV-enhanced green fluorescent protein. We successfully constructed the recombinant adeno-associated virus with the BMP-4/7 fusion gene. The transfection efficiency of AAV-BMP-4/7 was approximately 72% without significant biological effects on cell activity. Cell ossification was significant after

transfection with AAV-BMP-4/7. The 1×10^5 vg/cell multiplicity of infection value of transfection efficiency was more than 5×10^4 vg/cell (59.38%). Significantly higher ALP and OC activity occurred in the AAV-BMP-4/7 transfection groups than in the AAV-enhanced green fluorescent protein groups ($t_{\text{ALP}} = 896.88$, $P < 0.001$; $t_{\text{OC}} = 543.24$, $P < 0.01$). The AAV-BMP-4/7 fusion gene can highly efficient transfect rabbit BMSCs cultured *in vitro* and it has significant ossification activity.

Key words: Bone tissue engineering; Bone morphogenetic protein; Fusion gene; Adeno-associated virus; Bone marrow stromal cells

INTRODUCTION

Bone morphogenetic proteins (BMPs) can induce bone marrow stromal cells (BMSCs) to differentiate into ossification or chondroblasts and promote the formation of new bone. At present, the BMP family has more than 20 members, of which BMP-2, BMP-4, and BMP-7 have the strongest activity and can promote the formation of cartilage and new bone. Promoting the fusion of bone and spine has been successfully undertaken (Woo and Morrey, 1982; Mahoney and Pellicci, 2003). In these experiments, BMP-4 and BMP-7 have been shown to play various roles in promoting the fusion of bone and spine (Berry et al., 2004; Meek et al., 2006). The BMPs in the human body (hBMPs) are mostly homodimers, but a few, such as BMP-2/7 and BMP-4/7, are heterodimers. The literature reports that the activity of BMP heterodimers is 20 times that of homodimers (Kelley et al., 1998; Sanchez-Sotelo and Berry, 2001; Sultan et al., 2002; Forsythe et al., 2007).

The adeno-associated virus (AAV) is capable of the efficient transfection of target cells and long-term stable expression of foreign genes; it is also safe (National Joint Registry for England and Wales; <http://www.njrcentre.org.uk>). We constructed an AAV of the BMP-4/7 fusion gene (AAV-BMP-4/7) and observed the effects of its transfection on the biological behavior of rabbit BMSCs. The aim of this study was to determine whether a BMP-4/7 fusion gene promotes osteogenic activity in rabbit BMSCs and could provide a new treatment strategy for bone tissue engineering.

MATERIAL AND METHODS

Rabbit BMSC culture

Thirteen healthy male New Zealand rabbits were provided by the Central Laboratory of the First Hospital of Harbin Medical University. The rabbits weighed approximately 20 kg and were 2.5 months old. Rabbit BMSCs were isolated and cultured using the bone marrow method for primary culture. After the cells reached confluence into a monolayer for digestion and passage, third-generation cells that exhibited robust growth were collected for use in the experiment.

Plasmid construction

The primers of hBMP-4 and hBMP-7 genes were designed according to the mature peptide sequence. The BMP-4 primers were P1, 5'-CGGAATTCAACTTAATGAGGGAGG-

3' and P2, 5'-TTGGATCCGCTGCGGGAAGC-3'. The BMP-7 primers used were P1, 5'-TAG GATCCGCCGCGGGAGGATCCACG-3' and P2, 5'-AACTGCAGTAACTAGTGGCAG-3'. The *EcoRI* and *BamHI* sites were introduced upstream and downstream of the hBMP-4 gene. The *BamHI* and *PstI* sites were inserted upstream and downstream of the hBMP-7 gene. The complementary DNA (cDNA) sequences of hBMP-4 and hBMP-7 were amplified through one-step reverse transcriptase polymerase chain reaction (PCR) from placental tissue and were cloned into the pGEM-T vector to produce the recombinant plasmids pGEM-BMP-4 and pGEM-BMP-7, respectively. The 2 plasmids were digested with *EcoRI/BamHI* and *BamHI/PstI* enzymes and then ligated with T4 ligase at 16°C overnight. Transformation into *Escherichia coli* DH5 α followed to screen for positive clones, which were identified using *EcoRI/BamHI* and *BamHI/PstI* double-enzyme digestion, 1.5% agarose gel electrophoresis, and sequencing.

The BMP-4 and BMP-7 gene fragments were ligated to produce the BMP-4/7 fusion gene, which was then cloned into the pGEM plasmid identified through sequencing. The BMP-4/7 fusion gene was cleaved from pGEM-BMP-4/7, the recombination was completed in *E. coli*, and recombinant AAV (Vector Gene Technology Company Limited, China) was produced in 293 cells. To conduct *EcoRI*, *BamHI*, and *PstI* enzyme digestion identification and analysis, we transformed the AAV-BMP-4/7 plasmid into DH5 α . A large number of AAV plasmids were extracted, Lipofectamine 2000 (Promega, USA) was used to transfect the 293 cells according to manufacturer instructions, and G418 selection and culture were conducted to obtain a drug-resistant cloned cell line.

Cell morphology

After digestion with 0.25% trypsinase at 10⁵ cells on a 24-well plate, third-generation cells in good state were selected and inoculated. The cells were then cultured until 70% confluence and inoculated with the virus. Four groups with different multiplicity of infection (MOI) values of AAV transfection - namely 5 x 10⁴, 1 x 10⁵, 5 x 10⁵, and 1 x 10⁶ vg/cell - were selected for the experiment. Each group contained 6 wells. Based on the MOI values of the cells, the required amount of virus and serum Dulbecco's modified Eagle's medium were added into each well. The virus solution was aspirated 2 h after transfection and added to ordinary Dulbecco's modified Eagle's medium for conventional culture. The cell changes were observed every 24 h after transfection.

Cell proliferation activity

Rabbit BMSCs (transfected group) were transfected for 2 h with the virus at 1 x 10⁵ vg/cell MOI. The untransfected BMSCs were used as the control group. The cells were inoculated on a 96-well plate at 1 x 10⁴ cells/well after digestion and were collected after inoculation for 12, 24, 48, 72, and 96 h to determine cell activity using a 3-(4,5-dimethylthiazol-2-yl)-2,5-diphenyltetrazolium bromide assay ($\lambda = 630$ nm). A cell growth curve was constructed, and the cell proliferation states in the 2 groups were compared to observe the effect of AAV-BMP-4/7 transfection on cell proliferation.

The cells from the AAV-BMP-4/7-transfected group and AAV-EGFP (enhanced green fluorescent protein-transfected group), which was provided by VGTC Gene Technology Company Ltd., Beijing, China, were collected. After transfection for 7 and 14 days, the cells were observed under an

inverted phase contrast microscope. Seven days after transfection, the cell morphology had changed significantly. The cell distribution was uneven, showing partial intensive and local porosity. The cells were polygonal, and under high-power magnification, brown particles were seen in the cytoplasm, which indicated a significant osteogenic change. After 14 days, the cells showed multiple-layer growth, and the brown particles in the cytoplasm were more evident, which indicated calcium nodule formation in the cell. The AAV-EGFP group showed only cell contraction with irregular margins but no changes specific to osteogenic cell differentiation.

Transfection efficiency

Third-generation cells in good state were selected and, after 2 h of transfection with the virus at 1×10^5 vg/cell MOI, green fluorescence was detected through flow cytometry and the transfection efficiency of the cells was calculated (repeated six times). An MOI value of 5×10^4 vg/cell was used as the control.

Osteogenic activity

Cells were cultured for 7 and 14 days after transfection with AAV-BMP-4/7 for 2 h (experimental group). Morphological cellular changes and osteogenic differentiation were observed with an inverted phase contrast microscope. AAV-EGFP was used as the control group (6 samples each). Approximately 7 and 14 days after transfection, the supernatants from the 2 groups of cells were collected. Following manufacturer instructions on the alkaline phosphatase (ALP) assay kit (Boster Company, China), we conducted colorimetric determination (520-nm, 1-cm light path colorimetry), and the ALP content was measured in the supernatant. The supernatants of the 2 groups of cells were collected at 7 and 14 days after transfection, respectively. The osteocalcin (OC) values were tested according to manufacturer instructions (Immune Technology Institute of East Asia, Beijing, China). Approximately 100 μ L of the cell culture medium was mixed with 100 μ L 125 I-labeled OC antibodies and kept at 4°C for 24 h. Separated agent was then added and mixed to the solution, which was placed at room temperature and centrifuged at 4°C. The radiation dose of the detected precipitation in the supernatants was discarded, and the average OC content of each group was calculated (repeated 6 times).

Statistical analysis

The data were analyzed using SPSS 11.5 and are reported as means \pm SD. The differences between groups were analyzed by the *t*-test, which represented the independent samples of the 2 groups. A P value of <0.05 was considered to be statistically significant.

RESULTS

Plasmid construction

The pGEM-BMP-4 and pGEM-BMP-7 plasmids were extracted and identified through agarose gel electrophoresis and PCR primer expansion identification. Two bright bands of 374 and 451 bp were found. The sequencing result was consistent with the report in GenBank

(Nos. NM_001202.3 and BC008584.1) and the size of the mature peptide gene sequences of BMP-4 and BMP-7.

AAV-BMP-4/7 was successfully obtained. A band of 826 bp was observed through double-enzyme digestion. Two bright bands of approximately 374 and 451 bp on the agarose gel appeared after *EcoRI*, *Bam*HI, and *Pst*I identification and PCR primer expansion (Figure 1), which indicated that the fusion gene of BMP-4 and BMP-7 was successfully obtained. The AAV plasmid carrying the BMP-4/7 fusion gene was generated after recombination.

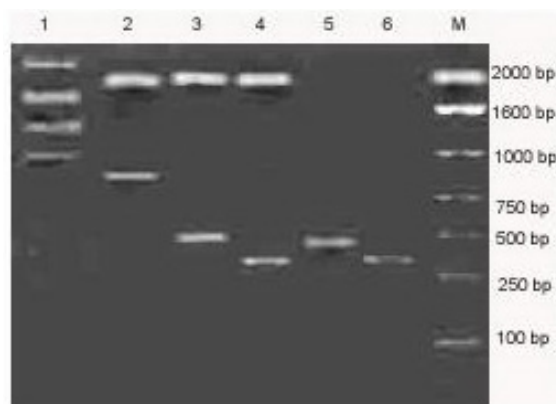


Figure 1. Adeno-associated virus (AAV) vector with bone morphogenetic proteins 4 and 7 (AAV-BMP-4/7) plasmid identification enzyme digestion. *Lane 1* = λ DNA molecular weight standard; *lane 2* = *EcoRI* and *PstI* enzyme digestion; *lane 3* = *Bam*HI and *PstI* enzyme digestion; *lane 4* = *EcoRI* and *Bam*HI enzyme digestion; *lane 5* = BMP-7 polymerase chain reaction-amplified fragment; *lane 6* = BMP-4 polymerase chain reaction-amplified fragment; *lane M* = DNA marker.

Cell morphology

Rabbit BMSCs were transfected with the virus at various MOI values. Approximately 24 h later, the cell morphology changed in each group, with long spindle cells contracting into irregular margins. The changes became significant after 72 h, and some cells lost the typical cell morphology of BMSCs. The cells began to show irregular arrangement in the form of polygons and random rectangles. These changes became more obvious with increasing MOI value. The 5×10^4 vg/cell group did not significantly change, the 1×10^5 vg/cell group changed minimally, and the 1×10^6 vg/cell group exhibited the most evident effect, in which some cells disintegrated (Figure 2).

Cells from the AAV-BMP-4/7-transfected group and AAV-EGFP-transfected group were collected. After transfection for 7 and 14 days, the cells were observed under an inverted phase contrast microscope. Seven days after transfection, the cell morphology changed significantly. The distribution of the cells was uneven, showing partial intensive and local porosity, and the cells were polygonal. Under high-power magnification, brown particles were seen in the cytoplasm, indicating significant osteogenic change. After 14 days, the cells showed multiple-layer growth, and the brown particles in the cytoplasm were more evident, indicating that calcium nodules had formed in the cells. The AAV-EGFP group showed only cell contraction and irregular margins and no specific changes of osteogenic cell differentiation (Figure 3).

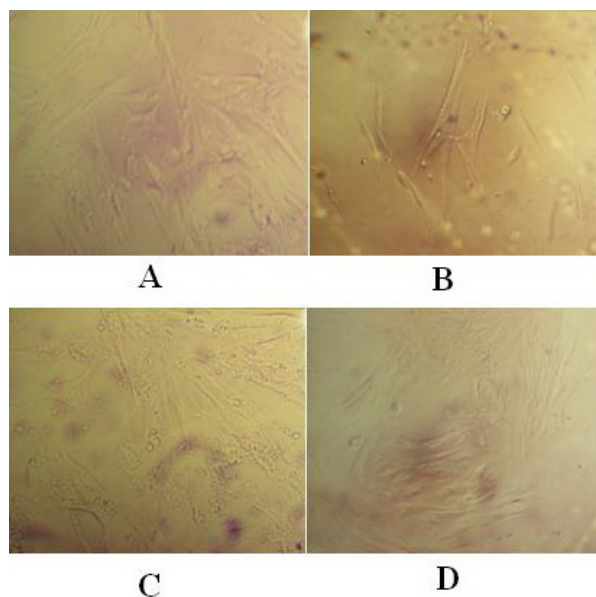


Figure 2. Cell changes after transfection with AAV-BMP-4/7 for 72 h. **A.** The 5×10^4 vg/cell group. **B.** The 1×10^5 vg/cell group. **C.** The 5×10^5 vg/cell group. **D.** Some cells in the 1×10^6 vg/cell group (200X).

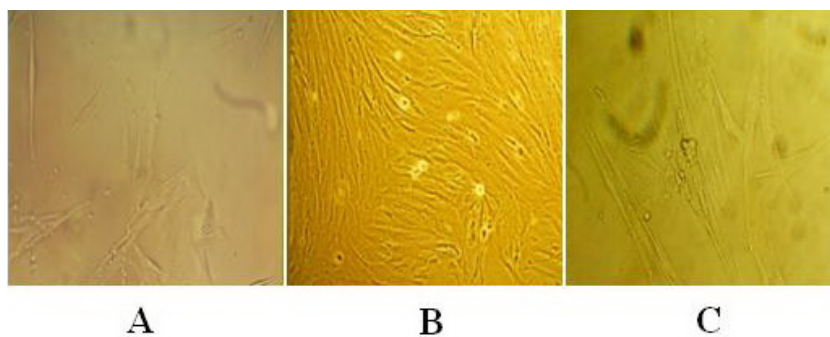


Figure 3. Cell morphological changes after transfection with AAV-BMP-4/7 under an inverted phase contrast microscope. **A.** Seven hours after transfection. **B.** Cells 14 days after transfection (200X). **C.** Cells in the AAV-enhanced green fluorescent protein-transfected group.

Cell proliferation activity

After inoculation for 12, 24, 48, 72, and 96 h, transfected and untransfected cells were assessed for activity using a 3-(4,5-dimethylthiazol-2-yl)-2,5-diphenyltetrazolium bromide method ($\lambda = 630$ nm). A cell growth curve was drawn. The result showed that the multiple proliferation periods of the 2 groups of cells both appeared at 24 h, and the activity of the transfected group was slightly lower than that of the untransfected group. However, the cell proliferation was active, which suggests that AAV had little effect on the cell growth curve (Figure 4).

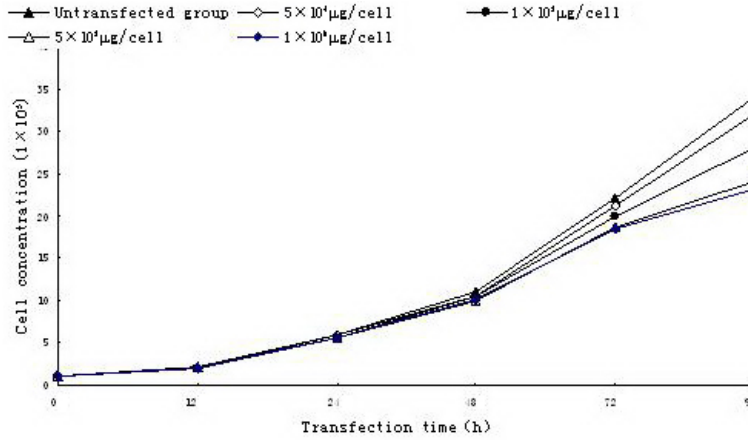


Figure 4. Growth curve of cells in the transfected and untransfected groups after inoculation for 12, 24, 48, 72, and 96 h.

Transfection efficiency

Third-generation cells in good state were selected, and after transfection by virus with an MOI value of 1×10^5 vg/cell, the transfection efficiency was calculated with flow cytometry. The average transfection efficiency was 72%. The MOI value of 1×10^5 vg/cell had a relatively minimal effect on cell morphology, but the transfection efficiency was more than that of cells transfected with virus having an MOI value of 5×10^4 vg/cell (59.38%; chi-square = 15.58, $P < 0.01$; Figure 5).

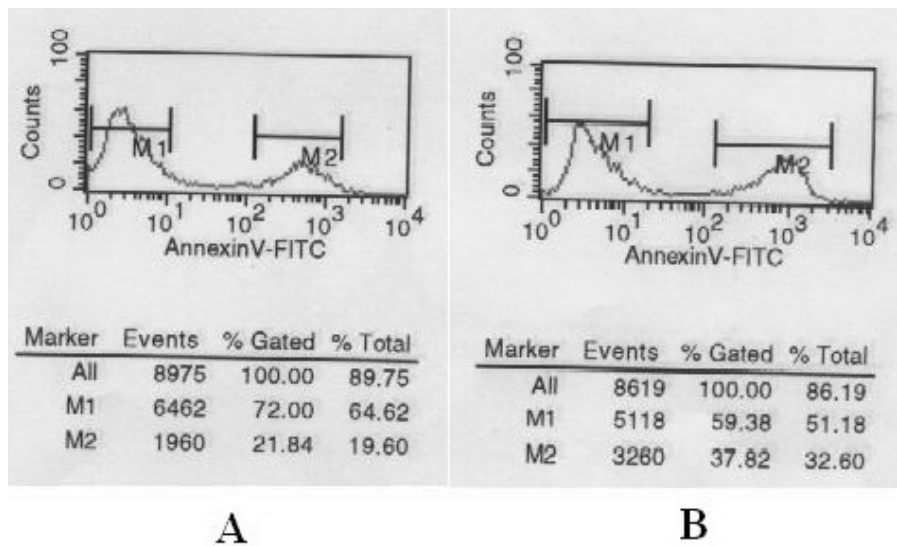


Figure 5. Transfection efficiency of bone marrow stromal cells transfected with AAV-BMP-4/7. **A.** Transfection with a multiplicity of infection value of 1×10^5 vg/cell. **B.** Transfection with a multiplicity of infection value of 5×10^4 vg/cell.

ALP content determination

Two groups of cells were selected for transfection. The cell supernatants were collected after 7 and 14 h to detect ALP concentration. The contents of the AAV-BMP-4/7 group was 67.2 ± 8.4 and 106.5 ± 12.1 Kim units, respectively, whereas the contents of the AAV-EGFP group were 10.1 ± 2.7 and 23.6 ± 4.8 Kim units, respectively. The difference between ALP contents of the AAV-BMP-4/7 group and the AAV-EGFP group was statistically significant ($t = 896.88$, $P < 0.001$).

OC content determination

Two groups of cells were selected for transfection. We collected the cell supernatants after 7 and 14 h to calculate OC contents. The concentrations of the AAV-BMP-4/7 group were 0.289 ± 0.014 and 0.363 ± 0.076 ng/mL, respectively, whereas those of the untransfected group were 0.011 ± 0.007 and 0.017 ± 0.010 ng/mL, respectively. The OC content difference between the transfected and the untransfected groups was statistically significant ($t = 543.24$, $P < 0.01$).

DISCUSSION

BMPs play a key role in the process of cell growth and bone formation; hence, they have been the focus of much research (Berry et al., 2005; Sanchez-Sotelo et al., 2006; Kung and Ries, 2007). The bone induction abilities of BMP-2, BMP-4, and BMP-7 (especially that of BMP-4) are the strongest among those of more than 20 BMPs. Recent studies have confirmed that the role of recombinant hBMP-4 in promoting spinal fusion is more prominent than that of recombinant hBMP-2, as its required dose is only one-tenth that of recombinant BMP-2, with the osteogenic volume being positively correlated with the dose (Aspenberg, 1998; Sundfeldt et al., 2006). Considering that BMP heterodimers have higher activity than that of homodimers *in vivo*, we selected BMP-4 and BMP-7 as target genes. The 2 mature peptide cDNA sequences were successfully cloned, and DNA recombinant technology was used to fuse the mature peptide cDNA of the BMP-4 and BMP-7 genes. The fusion gene was successfully cloned into a shuttle plasmid, and the AAV-BMP-4/7 plasmid was obtained after recombination in *E. coli*.

The AAV genome can be integrated into the DNA of the genome of the host cell, which ensures the long-term stable expression of foreign genes. The transcription elements in the AAV terminal repeated sequence do not fuse into the host DNA, and the likelihood of insertional mutagenesis is very small. The virus can also be integrated into cells during the division and nondivision phases and has a wide range of hosts (Robertsson et al., 1997; Alberton et al., 2002). Therefore, AAV can be used as a relatively suitable virus vector, which solves the problem of recombinant genes obtaining sustained expression through gene-engineering techniques. Currently, AAV is the basis of gene therapy and is one of the commonly used vectors in clinical research.

The difference in the MOI value of AAV-transfected cells was very large, ranging from 1×10^4 to 1×10^6 vg/cell. This result showed that an MOI of 1×10^5 vg/cell has little effect on cell morphology and has no obvious impact on cell proliferation activity. Its transfection

efficiency is 72%, significantly higher than the transfection efficiency of the general liposome at 20-30%. The MOI value of 5×10^4 vg/cell can achieve good transfection efficiency (55-65%), and its effect on cell proliferation activity is minimal (Paterno et al., 1997; Mahoney and Pellicci, 2003; Kwon et al., 2006). However, the results showed that an MOI of 1×10^5 vg/cell had higher transfection efficiency than that of an MOI of 5×10^4 vg/cell. The former can be used as the MOI of routine selection, which not only guarantees a certain amount of transfected virus but also ensures good transfection efficiency. The difference between our results and the transfection efficiency in the literature report was not statistically significant ($P > 0.05$) (Dong et al., 2007).

BMSCs are osteogenic stem cells that have the potential to differentiate into various cell lines. BMSCs can achieve cross-system differentiation under certain external environment and stimulating factors, are convenient to obtain and easy to culture, and are good sources of seed cells for tissue engineering (Amlie et al., 2010). AAV-BMP-4/7 was used to transfect the BMSCs, and the cell morphology changed from spindle to polygonal and cubic forms, showing obvious osteogenic changes. With extension of the transfection time, the changes in the features were more significant, and the difference was more dramatic compared with that in the control group. This finding indicated that the BMP-4/7 fusion gene had osteogenic activity and was positively correlated to transfection time.

BMPs play important roles in the osteogenic process - namely, the promotion of cell chemotaxis, mitosis, and cell differentiation (Hedlundh et al., 1996; Kelley et al., 1998; Bartz et al., 2000; Mahoney and Pellicci, 2003). The complicated process of BMSC differentiation into mature osteogenic cells occurs through the interactions of many system, paracrine, and autocrine factors. BMPs are added to the cultured BMSCs for induction. When the process of osteogenesis is induced, differentiation into osteogenic cells occurs. The cell synthesis and secretion express the osteogenic proteins and extracellular matrix components, such as ALP and OC, which are commonly used indicators of induction. The cell morphology showed that the cells transfected with AAV-BMP-4/7 had osteogenic activity after they were induced in the culture for 7 and 14 days. The activity gradually increased, whereas the AAV-EGFP control group showed no significant osteogenic activity. After transfection, AAV-BMP-4/7 was conducted and induced in the culture for 7 and 14 days. The ALP and OC contents in the supernatants both increased significantly with longer induced culture time. However, the ALP and OC contents in the AAV-EGFP control group did not increase significantly, so the results confirmed that the protein expressed by the BMP-4/7 fusion gene induced osteogenic activity after transfection via AAV.

In conclusion, we successfully constructed an AAV expression vector that contained a BMP-4/7 fusion gene. The results showed that the BMP-4/7 fusion gene was efficiently expressed in target cells via AAV and promoted the transformation of BMSCs to *in vitro* cells promoting bone formation.

REFERENCES

- Alberton GM, High WA and Morrey BF (2002). Dislocation after revision total hip arthroplasty : an analysis of risk factors and treatment options. *J. Bone Joint Surg. Am.* 84-A: 1788-1792.
- Amlie E, Hovik O and Reikeras O (2010). Dislocation after total hip arthroplasty with 28 and 32-mm femoral head. *J. Orthop. Traumatol.* 11: 111-115.
- Aspenberg P (1998). Wear and osteolysis in total joint replacements. *Acta Orthop. Scand.* 69: 435-436.

- Bartz RL, Nobel PC, Kadakia NR and Tullos HS (2000). The effect of femoral component head size on posterior dislocation of the artificial hip joint. *J. Bone Joint Surg. Am.* 82: 1300-1307.
- Berry DJ, von Knoch M, Schleck CD and Harmsen WS (2004). The cumulative long-term risk of dislocation after primary Charnley total hip arthroplasty. *J. Bone Joint Surg. Am.* 86-A: 9-14.
- Berry DJ, von Knoch M, Schleck CD and Harmsen WS (2005). Effect of femoral head diameter and operative approach on risk of dislocation after primary total hip arthroplasty. *J. Bone Joint Surg. Am.* 87: 2456-2463.
- Dong Z, Zheng Z and Kuang G (2007). Construction of recombinant adeno-associated virus vector with human bone morphogenetic protein. *Zhongguo Xiu Fu Chong Jian Wai Ke Za Zhi* 21: 738-742.
- Forsythe ME, Whitehouse SL, Dick J and Crawford RW (2007). Functional outcomes after nonrecurrent dislocation of primary total hip arthroplasty. *J. Arthroplasty* 22: 227-230.
- Hedlundh U, Ahnfelt L, Hybbinette CH, Wallinder L, et al. (1996). Dislocations and the femoral head size in primary total hip arthroplasty. *Clin. Orthop. Relat. Res.* 226-233.
- Kelley SS, Lachiewicz PF, Hickman JM and Paterno SM (1998). Relationship of femoral head and acetabular size to the prevalence of dislocation. *Clin. Orthop. Relat. Res.* 163-170.
- Kung PL and Ries MD (2007). Effect of femoral head size and abductors on dislocation after revision THA. *Clin. Orthop. Relat. Res.* 465: 170-174.
- Kwon MS, Kuskowski M, Mulhall KJ, Macaulay W, et al. (2006). Does surgical approach affect total hip arthroplasty dislocation rates? *Clin. Orthop. Relat. Res.* 447: 34-38.
- Mahoney CR and Pellicci PM (2003). Complications in primary total hip arthroplasty: avoidance and management of dislocations. *Instr. Course Lect.* 52: 247-255.
- Meek RM, Allan DB, McPhillips G, Kerr L, et al. (2006). Epidemiology of dislocation after total hip arthroplasty. *Clin. Orthop. Relat. Res.* 447: 9-18.
- Paterno SA, Lachiewicz PF and Kelley SS (1997). The influence of patient-related factors and the position of the acetabular component on the rate of dislocation after total hip replacement. *J. Bone Joint Surg. Am.* 79: 1202-1210.
- Robertsson O, Wingstrand H, Kesteris U, Jonsson K, et al. (1997). Intracapsular pressure and loosening of hip prostheses. Preoperative measurements in 18 hips. *Acta Orthop. Scand.* 68: 231-234.
- Sanchez-Sotelo J and Berry DJ (2001). Epidemiology of instability after total hip replacement. *Orthop. Clin. North Am.* 32: 543-52, vii.
- Sanchez-Sotelo J, Haidukewych GJ and Boberg CJ (2006). Hospital cost of dislocation after primary total hip arthroplasty. *J. Bone Joint Surg. Am.* 88: 290-294.
- Sultan PG, Tan V, Lai M and Garino JP (2002). Independent contribution of elevated-rim acetabular liner and femoral head size to the stability of total hip implants. *J. Arthroplasty* 17: 289-292.
- Sundfeldt M, Carlsson LV, Johansson CB, Thomsen P, et al. (2006). Aseptic loosening, not only a question of wear: a review of different theories. *Acta Orthop.* 77: 177-197.
- Woo RY and Morrey BF (1982). Dislocations after total hip arthroplasty. *J. Bone Joint Surg. Am.* 64: 1295-1306.